JOURNAL OF PROPULSION AND POWER
Vol. 17, No. 1, January–February 2001

Pressure Effects on Geometry and Structure of Gas Jet Flames in Crossflow

Ahsan R. Choudhuri* and S. R. Gollahalli†
University of Oklahoma, Norman, Oklahoma 73019

Flame structure and geometry of natural gas and propane diffusion flames in crossflow are presented to delineate the effects of buoyancy and ambient pressure. The fuel was injected horizontally into a vertically moving airstream. The buoyancy acted along the direction of the crossflow. The combustion-chamber pressure was varied from 1 to 1.45 bar and the crossflow to jet velocity ratio from 0.1 to 1.45. Quantitative rainbow schlieren deflectometry was used to visualize the flame and to measure the geometrical parameters. The centerline flame trajectory showed three distinct regions, and the dimensionless coordinate of the jet centerline in the jet direction varied with 0.45, 0.25, 0 power of the coordinate in the crossflow direction and −0.5 power of the Froude number based on the jet velocity in these regions. The flame trajectories did not change significantly with pressure. Flame chord length varied with 0.45 power of the crossflow/jet velocity ratio. Flame length and soot formation characteristics changed notably with pressure. Propane flames were more susceptible than natural gas flames to the ambient pressure. The flame luminosity caused by soot in the propane flame changed only slightly with velocity ratio. However, the natural gas flame became nonsooty at high velocity ratios.

Nomenclature

C	=	flame-tip chord length, $(y^2 + x^2)^{1/2}$
C_n	=	normalized flame chord length, $C/[d(\rho_0/\rho_j)^{1/2}]$
d	=	inside diameter of the burner
Fr	=	densimetric Froude number, $U_0^2\rho_j/[(\rho_j - \rho_0)gd]$
L	=	flame length
L_{lum}	=	luminous fraction of the flame length
L_{lumn}	=	normalized luminous fraction of the flame length, $L_{\text{lum}}/[d(\rho_0/\rho_j)^{1/2}]$
L_n	=	normalized flame length, $L/[d(\rho_0/\rho_j)^{1/2}]$
M	=	momentum flux, ρU^2
P	=	pressure
R	=	velocity ratio, U_0/U_j
$\mathcal{R}$	=	correlation coefficient
r	=	radius of the vortex core
U_j	=	fuel jet velocity
U_∞	=	crossflow velocity
W	=	characteristic schlieren boundary width
W_n	=	normalized $W = w/[d(\rho_0/\rho_j)^{1/2}]$
X	=	$x/[d(M_0/M_j)^{1/2}]$
x	=	horizontal axis length
Y	=	$y/[d(M_0/M_j)^{1/2}]$
y	=	vertical axis length
Γ	=	circulation of the vortex
ρ_j	=	fuel density
ρ_0	=	air density

Subscripts

j	=	conditions at the exit of fuel jet
0	=	crossflow conditions

Presented as Paper 99-2787 at the AIAA/ASME/SAE/ASEE 35th Joint Propulsion Conference and Exhibit, Los Angeles, CA, 20–24 June 1999; received 10 August 1999; revision received 9 April 2000; accepted for publication 9 April 2000.

*Research Assistant, Combustion and Flame Dynamics Laboratory, School of Aerospace and Mechanical Engineering. Student Member AIAA.

†Lesch Centennial Professor, Combustion and Flame Dynamics Laboratory, School of Aerospace and Mechanical Engineering. Associate Fellow AIAA.

Introduction

OVER the past few decades fluid mechanics and reaction kinetics of reacting fuel jets and flames in crossflow have been studied extensively through analytical, experimental, empirical, and semi-empirical models by several investigators.[1−5] Most of the analytical studies were concerned with the vortex interaction of a circular jet with the crossflow. The attempts to incorporate reaction kinetics into this model were successful only to a limited extent, and a number of assumptions were needed to simplify the flowfield. Experimental studies have focused on a wide variety of physical phenomena associated with a fuel jet burning in a crossflow including flame geometry, stability, and structure. However, these studies were done in a configuration where buoyancy acted normal to the crossflow.[6,7] As the momentum of crossflow was much higher than buoyancy, the effect of buoyancy was overshadowed and not clearly identifiable. Buoyancy plays an important role on flame structure, especially in hydrocarbon flames, particularly in the far-burner region.[1] Furthermore, the effects of burner wake were found to be significant on flowfield and flame dynamics.[1−3]

The present experimental study is aimed at identifying the relative effects of buoyancy on the flame geometry of a fuel jet burning in crossflow. To achieve this objective, the fuel jet was injected horizontally into a vertically moving crossflow in contrast to many of the previous studies where the jet was injected vertically into a horizontal crossflow. The densimetric Froude number was varied by changing the fuel. To understand the effects of ambient pressure, the chamber pressure was varied from 1 to 1.45 bar. The results are compared with the existing data, and differences have been discussed in light of the roles of buoyancy and pressure.

Background

A burning fuel jet issued from a circular burner protruding into a crossflow has a complex flowfield around it. The primary features of this flowfield are the aerodynamics of the fuel jet and the crossflow and their interaction with the burner. A number of studies are found in the literature related to the interaction of a round jet with a crossflow. Some theoretical models in literature emphasize the contrarotating vortex pair associated with the jet cross section and its influence on jet trajectory.[4,5] For a vertical jet in a horizontal crossflow, the vorticity component in the near field arises as a result of the deflection of the crossflow. A similar vortex behavior can be expected for the horizontal jet in a vertical crossflow. Furthermore, the horseshoe vortex system enhances the mixing in the near field

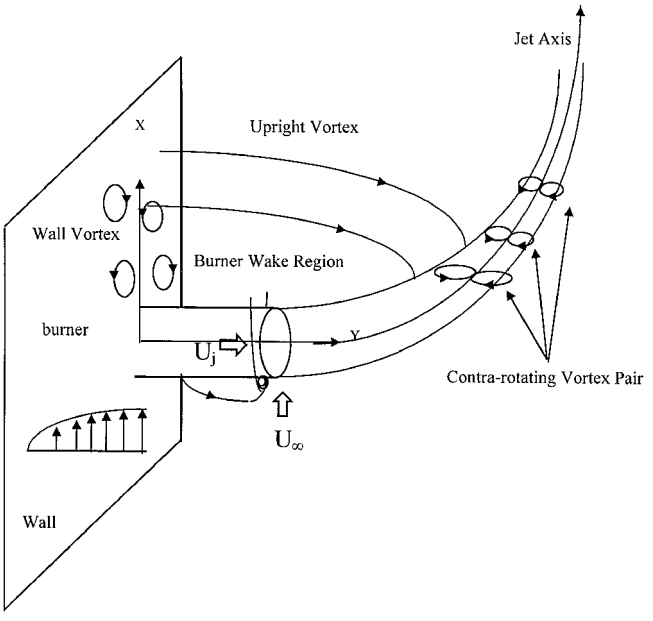

Fig. 1 Vortex system of fuel jet in crossflow.

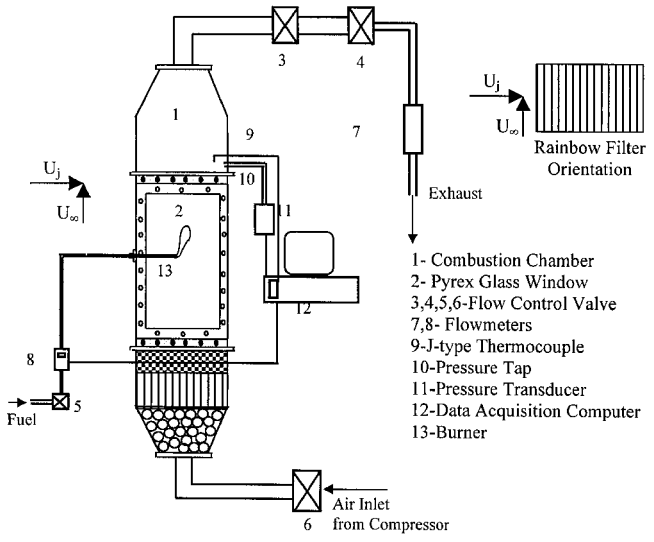

Fig. 2 Details of combustion chamber.

for both these cases. However, for a burning horizontal fuel jet issued into a vertical crossflow, the strength of the vortex system is expected to be higher because of the combined effects of crossflow and buoyancy, which act in the same direction.

For an isothermal upward vertical jet in a horizontal crossflow, the far field is dominated by a contrarotating vortex pair, which further grows in size as a result of the entrainment of crossflow. Buoyancy tends to deflect it only slightly. However, with a reacting horizontal jet in an upward moving crossflow, the combination of buoyancy with crossflow dominates the far field. As hot products accumulate in the far field, buoyancy accelerates the flow, and mass conservation requires narrowing of the streamlines. Hence, unlike an isothermal jet, the contrarotating vortex pair in a flame shrinks as it moves downstream. Thus, the prediction of flame geometry based on the isothermal jet model is not appropriate for the burning horizontal jet in a vertical crossflow system. Furthermore, heterogeneous combustion and nonlinear variation of heat release with fuel flow rate caused by soot burning in the far-burner region make the analytical prediction of flame geometry in that region more complicated.

Theoretically, the ambient pressure is not expected to have an effect on the trajectory of a jet in crossflow as long as the crossflow to jet momentum flux ratio remains constant. For a vortex system with a radius r and strength Γ, $P - P_\infty = -\rho_j \Gamma^2/8\pi^2 r^2$ (Ref. 8). Because density is directly proportional to pressure at a given temperature, the change in pressure does not result in a change of Γ for a constant initial jet impulse. Hence, the jet trajectory is expected to be independent of pressure. However, the flowfield of hydrocarbon flames in a crossflow is complicated by the heat release and heterogeneous combustion of soot particles. Therefore, the flame trajectory might be distorted with a change in ambient pressure as a result of pressure-chemical kinetics interaction.

A sketch of the flowfield for a horizontal fuel jet burning in an upwardly moving crossflow is shown in Fig. 1. The primary features of this flow system are the contrarotating vortex pair and their shrinkage downstream. The downstream wake regions of the jet and the burner contain a complex vortex system, which includes wall vortices on the vertical side of the test chamber and the horizontally oriented vortices shed by the burner tube. Experiments of the present study were designed to validate and to further increase our understanding of the aforementioned effects of buoyancy and ambient pressure on the flowfield of a jet flame in a crossflow.

Experimental Techniques

Experiments were carried out in a rectangular steel combustion chamber of 0.31 × 0.32 m square cross section and 0.76 m height. The chamber provided an optical access to the jet flowfield through two 40-cm wide Pyrex glass windows mounted on opposite walls. Air was supplied into the chamber from a high-pressure compressor through honeycombs and screens placed in the inlet diffuser. The pressure inside the chamber was controlled with two controlling valves located downstream of the chamber. The airflow rate was measured by a calibrated float-type rotameter. To maintain a certain crossflow velocity for a specific pressure, the flow control valves and the rotameter settings were adjusted simultaneously. The pressure and temperature inside the combustion chamber were monitored with a computer-controlled data acquisition system. A 300-mm-long stainless-steel tube burner of 2 mm i.d. and 3 mm o.d. with sharp edges was inserted horizontally through a vertical wall of the combustion chamber such that the tube protruded 145 mm from the wall. Thus the burner tip was located at the center of the combustion chamber and far away from the wall boundary layer, which ensured that the effects of wall vortices on the flame were negligible. The fuel flow system consisted of high-pressure natural gas and propane cylinders, digital flow meters, and needle valves. The details of the test chamber are shown in Fig. 2.

Quantitative rainbow schlieren deflectometry (RSD)[9–12] was used for flame visualization. For sooty hydrocarbon flames both flame boundary and schlieren boundary could be observed through this system. The RSD system is shown in Fig. 3a. Light (150-W continuous halogen light source connected with a 200-μm diam fiber optic cable) from a slit aperture (50 μm) was collimated using an achromatic lens (diameter = 63 mm, focal length = 490 mm) and deflected while passing through the flame caused by the variable density generated refractive index gradient. A decollimating achromatic (diameter = 63 mm, focal length = 490 mm) lens was used to refocus the light and to form a deflected source image on the filter plane. Another achromatic magnification lens was (diameter = 30 mm, focal length = 60 mm) used after the decollimating lens to magnify the image. The magnification lens was positioned such that a magnification factor of three could be achieved for better visualization. The filter was a transparent film with a computer-generated continuous spectrum colored rectangular strip. The filter was red in the center and yellow at the edges. Light was focused through the red region. Other colors appearing on the image showed the deflection of the incident light as a result of the refraction index gradient of the test medium. Although the flames in the present study were inherently three dimensional and the density associated refractive index had both horizontal and vertical gradients, the RSD filter was placed vertically to detect only the horizontal density-gradient field. The vertical gradients were significant only in a narrow region close to the flame deflection point, and the dominant density gradient of most of the flowfield was horizontal. The gray-tone version of the RSD filter is shown in Fig. 3b. The image was acquired with

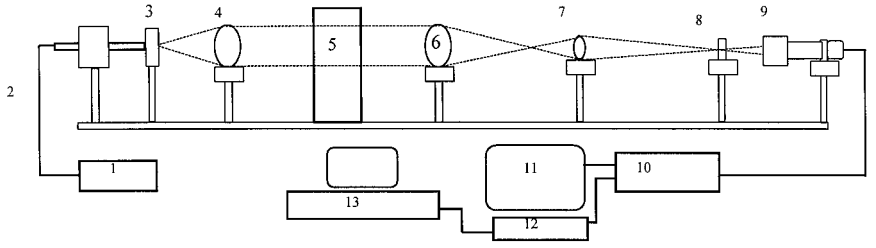

Fig. 3a Schematic of rainbow schlieren system. 1, light source; 2, fiber optic cable; 3, source apperture; 4, focusing lens; 5, test chamber; 6, refocusing lens; 7, magnifying lens; 8, rainbow filter; 9, CCD array; 10, camera controller; 11, monitor; 12, SVHS VCR; and 13, computer with frame grabber.

Fig. 3b Rainbow schlieren filter.

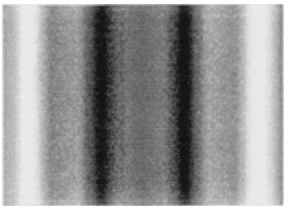

Table 1 Experimental conditions

Parameter	Value
Burner diameter	2 mm
Fuel	Hydrogen (95% + H_2, rest inert)
	Propane (95.35% C_3H_8, 2.98% CH_4, 0.92% C_2H_6, 0.73% C_4H_{18}, and remains are higher hydrocarbons)
	Natural Gas (95.8% CH_4, 1.19% C_3H_8, 1.15% C_2H_6, 0.50% CO_2, 0.10% N_2 and remains are pentane, hexane and water)
Jet velocity, U_j	0.15–0.5 m/s
Velocity ratio, U_0/U_j	0.396–1.37
Jet exit Reynolds number[a]	60–120
Densimetric Froude number[b]	2.5–10.66
Chamber pressure	1–1.45 bar
Chamber temperature	295–298 K

[a]Based on burner diameter and jet exit velocity.
[b]Based on burner diameter and crossflow velocity.

a charge-coupled device detector (Panasonic U-502) and recorded on a fiber optic coupled Super VHS video recorder. The image was grabbed off-line using a high-speed color frame grabber (Matrox) in red, green, and blue (RGB) format. In this experiment 25-ms time width was used to grab each image frame. The deflection of light could be quantified using the color attributes of the schlieren image. The color attributes were given by the strength of RGB and are quantifiable using HSI (hue, saturation and intensity) model.[9–12] The experimental conditions are listed in Table 1.

Results and Discussion

Flame Appearance and Structure

Both flame appearance and structure changed with the change of crossflow/jet velocity ratio R and test chamber pressure. The gray-tone versions of the rainbow schlieren photographs of the flames at different R and chamber pressures for natural gas and propane fuels are shown in Figs. 4a–4c. The color photographs are available in Choudhuri and Gollahalli.[13] The colors appearing in the pictures represent the density gradients across the flame. Although in a diffusion flame the density distribution is complex, in general, it represents the combined effects of temperature and concentration fields. For the natural gas flames at $R = 0.45$, flame appearance changed markedly when the ambient pressure was changed from 1 to 1.45 bar. The increase in luminous soot region (primarily visible radiation from burning solid carbon particles) with pressure indicates the change in the dominant reaction mechanism. The hydrocarbon oxidation at high pressure in a diffusion flame is markedly different from that at low pressure. Formation of intermediate carbon atoms in hydrocarbon diffusion flames increases with the increase of pressure.[14]

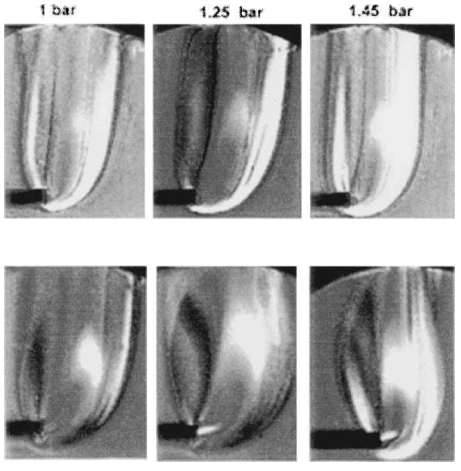

Fig. 4a Schlieren images of the flames at $R = 0.45$: top row, natural gas and bottom row, propane.

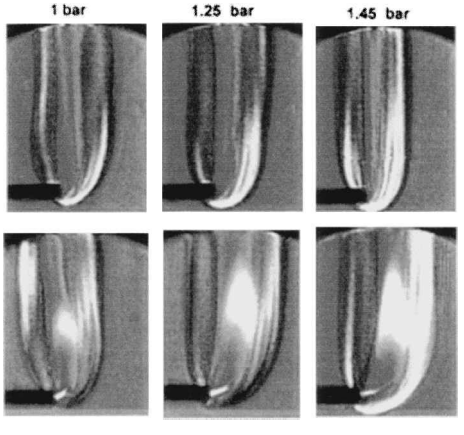

Fig. 4b Schlieren images of the flames at $R = 0.98$: top row, natural gas and bottom row, propane.

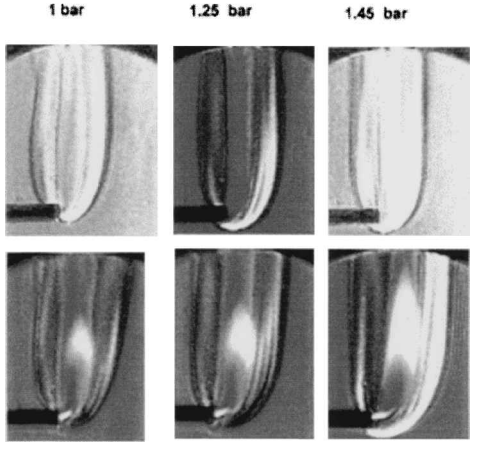

Fig. 4c Schlieren images of the flames at $R = 1.2$: top row, natural gas and bottom row, propane.

As a result, soot inception is enhanced through the formation of polycyclic aromatic hydrocarbon (PAH) as a result of increased isolation of carbon atoms. Soot particles cannot diffuse outward from the gaseous core, and hence combustion proceeds through the diffusion of the oxidizer. However, an increase of crossflow velocity increases the air entrainment into the flame and the availability of oxidizer in the fuel core, which suppresses the effect of pressure on soot formation. This is evident from the natural gas flames at higher R (0.98 and 1.2), where almost no soot is formed. In propane flames soot formation increases with pressure. However, the effect of the increase in crossflow velocity is not enough to mask the effects of pressure on soot inception and growth in a propane flame. The higher carbon/hydrogen (C/H) atom ratio of propane causes the rapid inception and growth of soot particles despite the increase of crossflow-enhanced mixing of fuel with air. This is the reason that soot formation in a propane flame is relatively independent over the range of R in the present experiment.

The boundaries of schlieren images reveal different types of mixing on the burner-wake side and crossflow side of the flame. The wake of the burner enhances mixing in the flowfield. In the natural gas flame at 1 bar and $R = 0.45$ (Fig. 4a), the burner wake side has primarily a single shade, which indicates comparatively uniform density. The strong mixing inside the burner wake keeps the density as well as the temperature uniform over a wide area. As the chamber pressure increases, this region spreads outward. With the increase in crossflow velocity, the density gradient becomes steeper as a result of a smaller turbulent wake region.[15] The freestream (crossflow) side of the flame has a more continuous density distribution, which indicates a slower mixing in this region. The effect of pressure on mixing cannot be identified explicitly from the schlieren image because of simultaneous changes of density with pressure and mixing. However, by digitally (pixel by pixel) subtracting the values of the hue at the boundaries of the atmospheric pressure images from those of the high-pressure images, it is found that in general, the increase in pressure somewhat slows mixing.

Centerline Trajectory

The relation between dimensionless coordinates X and Y following Gollahalli et al.,[1] which define the centerline of the flame, is shown in Fig. 5. The centerline was considered as the locus of the midpoints of the local diameter measured normal to the visible boundaries. Unlike the other measurements reported in the literature on the trajectories of vertical jet flames in a horizontal crossflow,[1] the flame trajectories in this case have three distinct regions. In the near field, where the jet momentum is dominant, the trajectories are correlated with $Y \sim X^{0.5}$, which is the same as the measurements reported in experiments where buoyancy acts normal to the crossflow. In the present investigation buoyancy is aligned with the crossflow, and hence the flame is expected to be bent more quickly than in earlier studies. However, in the near-burner region as a result of the dominance of jet momentum, the effect of buoyancy is not significant. Between the far downstream and the near-field region a small transition zone exists where the jet momentum starts to weaken, and the crossflow momentum and buoyancy dominate the flowfield. In previously reported measurements caused by the counteracting effects of crossflow and buoyancy, the flame trajectories had higher slopes (dY/dX) and followed the well-known third power law ($Y \sim X^{0.3}$) (Refs. 1 and 4). However, in the present study the buoyancy vector is aligned with crossflow and enhances its strength. Hence, the slope

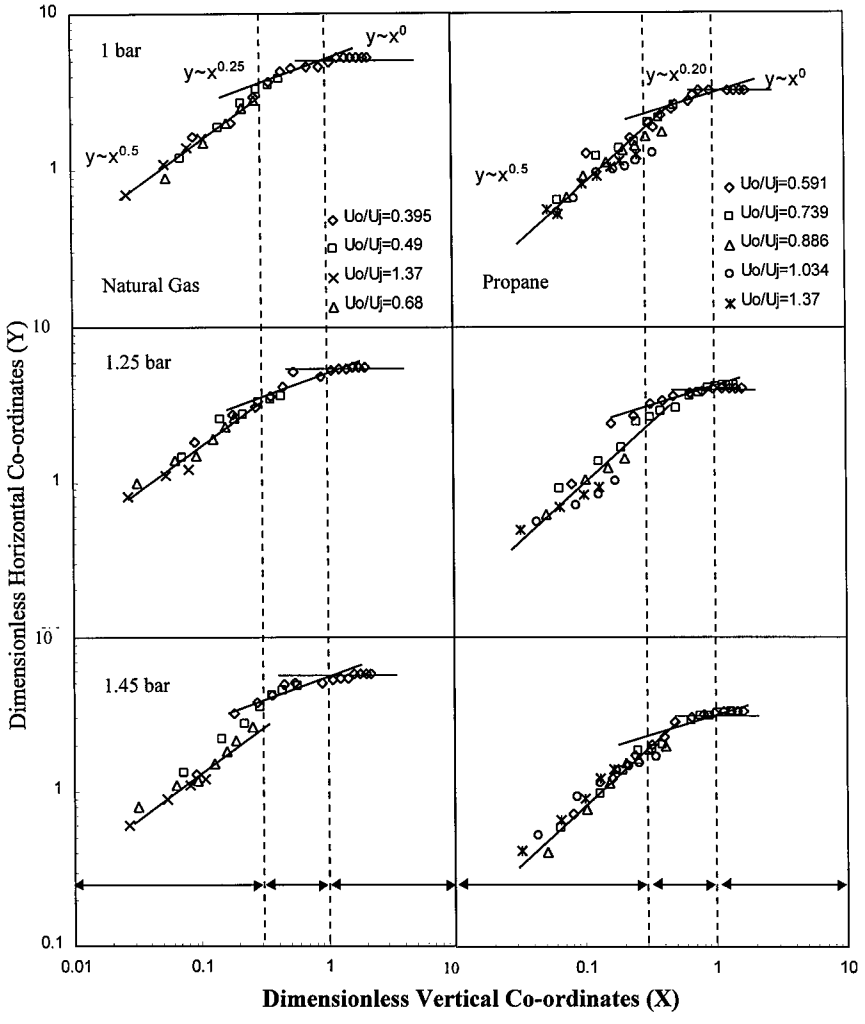

Fig. 5 Effects of pressure and fuel type on centerline trajectory of the visible flame (Maximum estimated uncertainties at 95% confidence interval based on t test; for X: ± 3% of the mean value and for Y: ± 3.8% of the mean value).

of the flame trajectories is smaller compared to those in the earlier measurements. In this region the flame trajectory has a correlation of $Y \sim X^{0.25}$ and $Y \sim X^{0.2}$ for natural gas and propane flames, respectively. In the far downstream, where mostly the postcombustion gases exist, the buoyant force is significant. Contrary to the cold-jet data in the literature, the flame trajectories do not follow the third power because of the effect of buoyancy.[1] In the present investigation, because buoyancy acts together with the crossflow, the flame trajectories are completely bent toward the vertical direction and are aligned with the crossflow, yielding the $Y \sim X^0$ correlation.

Although test chamber pressure has significant effects on the thermochemistry of flame, the flame trajectory is independent of ambient pressure changes as long as the momentum-flux ratio is constant. This indicates that the flame trajectory is mainly dependent on fluid mechanics.

The effect of densimetric Froude number on flame trajectory becomes significant as a result of buoyancy. This effect is especially notable in the transitional zone where most of the fuel burns and the jet momentum and buoyancy are comparable. The flame trajectories normalized by a function of Froude number for the two fuels are shown in Fig. 6. In the transitional region the flame trajectory data of both fuels collapse into a single correlation $Y \sim X^{0.25} Fr^{-0.5}$ with a correlation coefficient $\mathcal{R} = 0.96$.

Flame Chord Length

The variation of the normalized flame chord length of the arc of the flame centerline trajectory C_n with velocity ratio R is shown in Fig. 7. The chord length is defined as $(y^2 + x^2)^{1/2}$, where x and y are obtained at the flame tip (furthest point of the visible flame). Generally, the flame chord length varies with the crossflow to jet velocity ratio according to the relation $C_n \sim R^a$. In literature experimental and computational studies reported that the value of a is approximately 0.5 (Refs. 4 and 5). This relation presumably considers the invariance of chord length with densimetric Froude number and pressure. However, these predictions do not account for soot formation and oxidation in the flame. In fact, some investigators[16,17] contradict the theoretical prediction and found that the flame length is indeed dependent on ambient pressure except for very large flames where diffusion is not the only rate-limiting process. In the present investigation the value of a is found to be 0.45, slightly lower than that in the literature. The reason for this lower value is the combined effect of buoyancy and crossflow acting colinearly in the present study. As was discussed earlier, all of the previous investigations were conducted in a configuration where buoyancy acted normal to the crossflow, and hence the buoyancy effect was somewhat mitigated by the crossflow. Because in the present investigation the buoyant force and the crossflow momentum act together in the same direction, the fuel jet bends faster than in the earlier investigations. Also, despite the increase in chord length with pressure, the trend in the variation of chord length with velocity ratio R remains the same at all pressures.

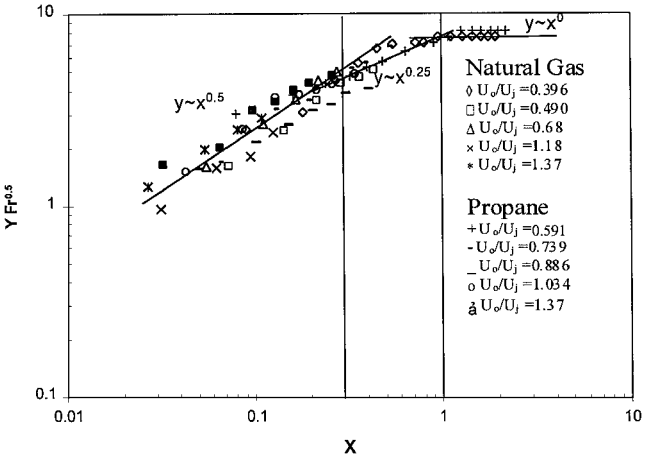

Fig. 6 Centerline trajectory correlations in different regions of flame in crossflow.

Flame Length

The effects of crossflow on visible flame length, measured along the curvilinear centerline, at different pressures for natural gas and propane flames are shown in Fig. 8. In general, the flame length increases with the increase in crossflow velocity. As the crossflow velocity increases, the flame quickly bends over and is convected downstream. The increase in crossflow velocity enhances entrainment in the near-burner region and is expected to result in shorter flames. However, the effect appears to be compensated by the lower air entrainment in the bent-over portion of the flame, which behaves like a flame in a coflow, and hence the flame is elongated with the increase in crossflow velocity.

According to Roper,[18] the length of a vertical and confined laminar diffusion flame should be independent of pressure at constant fuel mass-flow rate both for equal and unequal fuel-air velocities. However, some experimental investigations contradict Roper's prediction.[16,17] Because the theoretical prediction of Roper[18] does not account for the soot formation in the flame, it is believed that the increase of soot formation rate with the increase of pressure is largely responsible for the disagreement of experimental measurements with theoretical predictions. As pressure increases, the rate of complex fuel pyrolysis reactions in a hydrocarbon flame increases, which results in a larger soot formation and longer flames. In this investigation a similar trend is observed. For propane, flame length increases with pressure, particularly at high value of R. However,

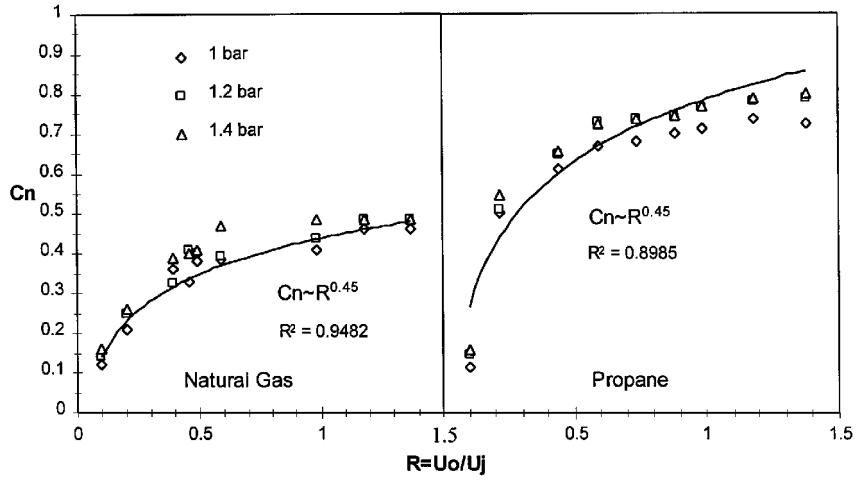

Fig. 7 Variation of flame chord length with velocity ratio and pressure (Maximum estimated uncertainties at 95% confidence interval based on *t* test; for C_n: ± 3.6% of the mean value).

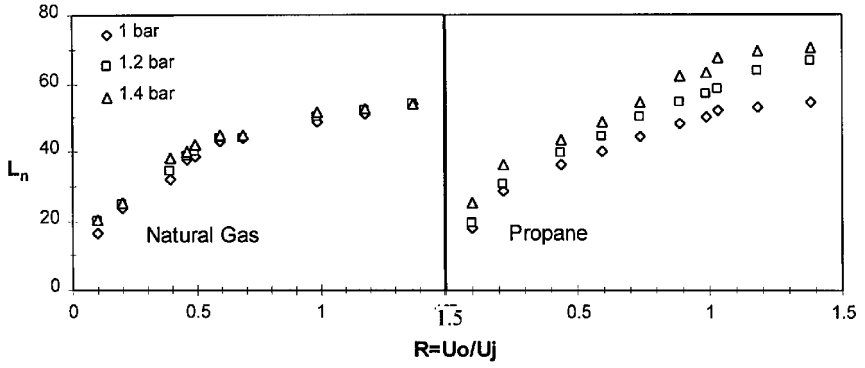

Fig. 8 Variation of curvilinear flame length with velocity ratio and pressure (Maximum estimated uncertainties at 95% confidence interval based on *t* test; for L_n: ± 3.4% of the mean value).

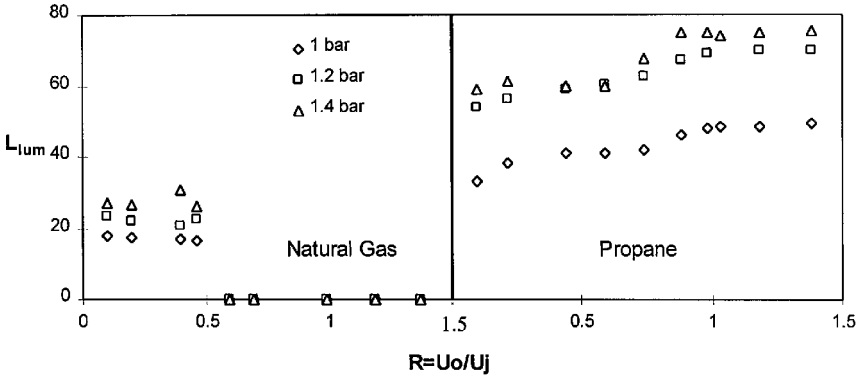

Fig. 9 Variation of luminous flame fraction with velocity ratio and pressure (Maximum estimated uncertainties at 95% confidence interval based on *t* test; for L_{lum}: ± 3.8% of the mean value).

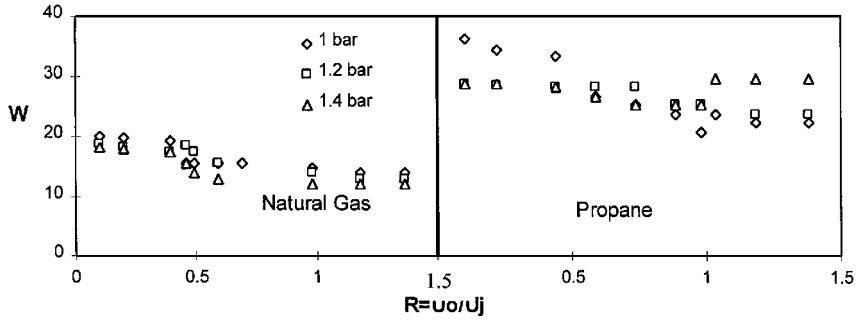

Fig. 10 Variation of maximum characteristics schlieren boundary width with velocity ratio and pressure (Maximum estimated uncertainties at 95% confidence interval based on *t* test; for *W*: ± 4% of the mean value).

the increase in flame length for natural gas appears insignificant, which can be attributed to inherently less sooty nature of natural gas flames.

Extent of the Luminous Flame Region

The extent of the luminous flame region in terms of the percent luminous fraction L_{lum}, following Gollahalli et al.,[1] of the flame length is shown in Fig. 9. It is expected that propane flames produce much higher soot than natural gas flames because of a higher C/H atom ratio in the fuel. An increase in crossflow velocity causes the natural gas flames to become nonsooty because of the increased mixing of fuel and oxidizer at a high crossflow velocity. On the other hand, for propane fuel the luminous fraction of the flame initially increases and then decreases as the crossflow velocity increases. Because the propane flame is inherently sooty, initially the increased mixing caused by a higher crossflow velocity is not adequate to reduce the effect of soot. However, for a much higher crossflow velocity the increased mixing dominates the process, and hence the sooty fraction of the flame does not increase significantly. As discussed earlier, the increase of soot concentration in hydrocarbon diffusion flames with pressure is a well-known phenomenon. This effect is also observed here. For propane flames luminous sooty part increases with pressure. However, L_{lum} decreases with pressure in natural gas flames. Unlike in typical vertical diffusion flames, propane flames in crossflow have a larger blue near-burner region, which indicates an increased mixing of fuel and oxidizer.

Maximum Characteristic Schlieren Boundary Width

The variation of the maximum characteristic schlieren boundary width *W*, measured (along a normal to the centerline) as the distance between points where color attains the background color corresponding to the undisturbed flowfield, at different velocity ratios and chamber pressures for natural gas and propane flames is shown in Fig. 10. Schlieren boundary width decreases with the increase of

both velocity ratio and pressure. The increase of velocity ratio affects the characteristic schlieren boundary width in two ways. First, the reacting species are convected downstream quickly, which results in an increase of flame length and a decrease in width. On the other hand, because the fuel-air mixing rate increases with the increase of velocity ratio R, the combustion of fuel becomes confined to a smaller zone. The characteristic schlieren width of natural gas flames slightly decreases with pressure because of the stretching of the streamlines. However, because the fuel density also increases with pressure, the effect of stretching is minor. Interestingly, in propane flames the schlieren boundary width actually increases with pressure. An increase in flame volume caused by solid particles might also cause this increment. However, that increase is insignificant compared to the schlieren boundary change with velocity ratio.

Conclusions

1) The centerline trajectories defined by the dimensional coordinates X and Y show three distinct regions. In the near-burner region, where jet momentum is dominant, the correlation agrees with cold jet data ($Y \sim X^{0.5}$). In the far-burner region, where buoyancy is significant and collinear with crossflow, the correlation is $Y \sim X^{0}$. Between these two extremes, in the midflame transitional region, the correlation shows $Y \sim X^{0.25}$ (natural gas) and $Y \sim X^{0.2}$ (propane) dependence compared to $Y \sim X^{0.28}$, where buoyancy was normal to crossflow. Further, while incorporating the Froude number, the data collapse for natural gas and propane flames into a single relation $Y \sim X^{0.25} Fr^{-0.5}$ in the transitional region.

2) The variation of flame chord length with velocity ratio in the present study is different from previous studies, where buoyancy acted normal to the crossflow direction. The variations in pressure and densimetric Froude number change the magnitude of the flame chord length; however, its trend with velocity ratio remains constant.

3) The visible curvilinear flame length increases with velocity ratio and pressure.

4) In a natural gas flame the luminous soot region decreases with the increase of velocity ratio; however, in a propane flame it initially increases with velocity ratio and subsequently remains constant.

5) The maximum characteristic schlieren boundary width decreases with the increase in velocity ratio for both natural gas and propane flames. With the increase in ambient pressure, the characteristic schlieren boundary width decreases in the natural gas flame, whereas it increases in the propane flame.

Acknowledgment

This research was supported by NASA Microgravity Research Division Grant NAG 3-1594. The authors thank the contract monitor De Von Griffin of the NASA John H. Glenn Research Center at Lewis Field.

References

[1]Gollahalli, S. R., Brzustowski, T. A., and Sullivan, H. F., "Characteristics of a Turbulent Propane Diffusion Flame in a Cross Wind," *Transaction of The Canadian Society of Mechanical Engineers*, Vol. 3, No. 4, 1976, pp. 205–213.

[2]Gollahalli, S. R., and Nanjundappa, B., "Burner Wake Stabilized Gas Jet Flames in Cross-Flow," *Combustion Science and Technology*, Vol. 109, No. 1–6, 1995, pp. 327–346.

[3]Huang, Rong F., and Wang, Show M., "Characteristics Flow Modes of Wake-Stabilized Jet Flames in a Transverse Air Stream," *Combustion and Flame*, Vol. 117, No. 1–2, 1999, pp. 59–77.

[4]Broadwel, J. E., and Breidenthal, R. E., "Structure and Mixing of a Transverse Jet in Incompressible Flow," *Journal of Fluid Mechanics*, Vol. 148, 1984, pp. 405–412.

[5]Kelso, R. M., Lim, T. T., and Perry, A. E., "An Experimental Study of Round Jet in Cross-Flow," *Journal of Fluid Mechanics*, Vol. 306, 1996, pp. 111–114.

[6]Huang, R. F., and Chang, J. M., "The Stability and Visualized Flame and Flow Structures of a Combusting Jet in Cross Flow," *Combustion and Flame*, Vol. 98, No. 3, 1994, pp. 267–278.

[7]Huang, R. F., and Yang, M. J., "Thermal and Concentration Fields of Burner-Attached Jet Flames in Cross Flow," *Combustion and Flame*, Vol. 105, No. 1–2, 1996, pp. 211–224.

[8]Bertin, J. J., and Smith, M. L., *Aerodynamics for Engineers*, 3rd ed., Prentice–Hall, Upper Saddle River, NJ, 1998, pp. 88, 89.

[9]Shenoy, A. K., Agrawal, A. K., and Gollahalli, S. R., "Quantitative Evaluation of Flow Computation by Rainbow Schlieren Deflectometry," *AIAA Journal*, Vol. 36, No. 11, 1998, pp. 1953–1960.

[10]Al-Ammar, K., Agrawal, A. K., Gollahalli, S. R., and Griffin, D., "Application of Rainbow Schlieren Deflectometry for Concentration Measurements in an Axisymmetric Helium Jet," *Experiments in Fluids*, Vol. 25, No. 2, 1998, pp. 89–95.

[11]Rohmat, T. A., Katoh, H., Obara, T., Yoshihashi, T., and Ohyagi, S., "Diffusion Flame Stabilized on a Porous Plate in a Parallel Air Stream," *AIAA Journal*, Vol. 36, No. 11, 1998, pp. 1945–1952.

[12]Agrawal, A. K., Nelson, K. B., Gollahalli, S. R., and Griffin, D., "Three-Dimensional Rainbow Schlieren Tomography of Temperature Field in Gas Flows," *Applied Optics*, Vol. 37, No. 3, 1998, pp. 479–485.

[13]Choudhuri, A. R., and Gollahalli, S. R., "Effects of Ambient Pressure and Burner Scaling on Geometry and Structure of Gas Jet Flames in Cross-Flow," School of Aerospace and Mechanical Engineering, Univ. of Oklahoma, Research Rept. OU-AME-2000-1, Norman, OK, March 2000.

[14]McArragher, J. S., and Tan, K. J., "Soot Formation at High Pressures: A Literature Review," *Combustion Science and Technology*, Vol. 5, No. 5, 1972, pp. 257–261.

[15]Shizawa, T., Honami, S., and Miyauchi, K., "Near Wall Vortex Structures in an Inclined Wake," AIAA Paper 98-0441, Jan. 1998.

[16]Miller, I. M., and Maahs, H. G., "High-Pressure Flame System for Pollution Studies with Results for Methane-Air Diffusion Flames," NASA TN D-8407, June 1977.

[17]Parker, W. G., and Wolfhard, H. G., "Carbon Formation in Flames," *Journal of the Chemical Society*, 1950, pp. 2038–2049.

[18]Roper, F. G., "The Prediction of Laminar Jet Diffusion Flame Sizes: Part I, Theoretical Model," *Combustion and Flame*, Vol. 29, No. 3, 1977, pp. 219–226.